



# Development of a novel solid phase microextraction calibration method for semi-solid tissue sampling

Ruifen Jiang<sup>a,\*</sup>, Wei Lin<sup>b</sup>, Lifang Zhang<sup>a</sup>, Fang Zhu<sup>b</sup>, Gangfeng Ouyang<sup>b</sup>

<sup>a</sup> Guangdong Key Laboratory of Environmental Pollution and Health, School of Environment, Jinan University, Guangzhou 510632, China

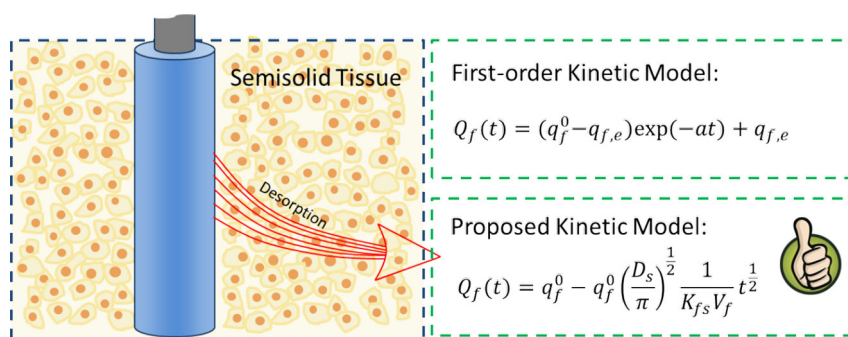
<sup>b</sup> KLGHEI of Environment and Energy Chemistry, School of Chemistry, Sun Yat-sen University, Guangzhou 510275, China



## HIGHLIGHTS

- A new extraction kinetic model was proposed for SPME semisolid sampling.
- A novel calibration method was developed for SPME semisolid sampling.
- The effect of complexity on sampling kinetic was thoroughly evaluated
- The feasibility of the proposed calibration method was demonstrated by fish tissue.

## GRAPHICAL ABSTRACT



## ARTICLE INFO

### Article history:

Received 28 September 2018

Received in revised form 14 November 2018

Accepted 15 November 2018

Available online 17 November 2018

Editor: Jay Gan

### Keywords:

SPME

Sampling kinetic

On-fiber standard calibration

Performance reference compound

*In vivo* SPME

## ABSTRACT

Accurate quantitative analysis using *in vivo* solid phase microextraction (SPME) for semi-solid tissue can be challenging due to the complexity of the sample matrix. In this paper, a comprehensive study was carried out on the extraction kinetics of SPME in the semi-solid sample, and subsequently proposed a new theoretical model to interpret the kinetic extraction process. Theoretically derived mathematical expressions well described the experimental desorption time profiles of the SPME process. Modelling experiments were also carried out to study the effect of sample tortuosity and binding matrix on the parameters affecting the extraction kinetics. Seven polyaromatic hydrocarbons (PAHs) and eight polychlorinated biphenyls (PCBs) in agarose gel and in real fish tissue were used for these experiments. The experimental data showed excellent agreement with theoretical prediction while providing excellent interpretation of the effect of tortuosity and binding matrix. Based on the theoretical model, an on-fiber standard calibration method with fewer internal standards was developed. The newly developed calibration method was used to quantify PAHs and PCBs in agarose gel and fish tissue. By using the proposed calibration method, a large number of organic compounds can be quantified with fewer internal standards. Current study provides the theoretical foundation for *in vivo* SPME quantitative semi-solid tissue analysis in the future.

© 2018 Elsevier B.V. All rights reserved.

## 1. Introduction

Since its introduction in 1989, solid phase microextraction (SPME) has been well accepted by the analytical chemistry community due to its miniaturized format, the ability for high throughput analysis, minimal need for organic solvent (Pawliszyn, 2012), and the combination

\* Corresponding author

E-mail address: [jiangrf5@jnu.edu.cn](mailto:jiangrf5@jnu.edu.cn) (R. Jiang).

of sampling and sample preparation into a single step. The technique has been well applied to gas, aqueous and solid sample analysis. Among them, *in vivo* sampling has gained more attention due to its unique format and convenient design (Ouyang et al., 2011b). *In vivo* sampling approach has been used for studying the environmental fate of organic pollutants in animal and plant (Chen et al., 2015; Xu et al., 2014b); monitoring the volatile and semi-volatile emissions from micro-organisms, insects, plants, and human breath (Augusto and Luiz Pires Valente, 2002; Bessonneau et al., 2017); quantitative analysis of targeted compounds (Roszkowska et al., 2018a, 2018b) and qualitative screening the non-targeted compounds in metabolomics studies (Lord et al., 2011).

Like any quantitative method, SPME is a non-exhaustive sampling technique that requires calibration to correlate the extracted amount to the original concentration of analytes in the sample matrix. Although *in vivo* SPME has been widely applied, accurate quantitative analysis can still be challenging, especially for the semi-solid samples (Ouyang et al., 2011b, 2011a; Roszkowska et al., 2018a, 2018b). Some of the reasons for the challenge may be due to vague theoretical model for the extraction kinetic process in the semi-solid sample, in which the first-order kinetic model has been commonly used to describe the sampling kinetics of SPME. However, Xu et al. (2016b) pointed out that the sampling kinetics in semi-solid sample was different for aqueous and gaseous systems, where the mass transfer process was dominated by convection, and the boundary layer between the SPME fiber surface and bulk sample. Thus, using the first-order kinetic model to describe the kinetic process may be inaccurate for a semi-solid sampling process. It is important to note that in the semi-solid sample, diffusion process usually dominate the mass transfer whereas convection is negligible. Thus, diffusion in the tissue matrix and the fiber coating are the rate-limiting steps for SPME, and the kinetic process was not likely a first order process.

Besides the extraction kinetic model of SPME, the intrinsic complexity of the semi-solid sample may also affect accurate quantification of analytes (Zhang et al., 2011b, 2011a, 2010a, 2010b). The complexity of sample matrix includes the tortuosity and protein/lipid binding matrices that would cause variation on mass transfer of the analytes. Although, research has been carried out to investigate the effect of binding matrix on the aqueous sampling (Jiang et al., 2015b; Xu et al., 2016a), limited work has been done on semi-solid sampling, especially on the analytes kinetic processes. Zhang et al. (2011a) first studied the effect of the sample tortuosity and binding matrices on the kinetics of analytes during sampling. The study indicated that the tortuosity of the tissue could influence the diffusion path of the chemicals, while the binding matrix affected the chemicals distribution constant between the sample and the SPME fiber coating. Moreover, the authors proposed that kinetic calibration method based on loaded fiber with stable isotope or performance reference compounds (PRC) can be employed to correct the variation caused by the sample tortuosity and the matrix binding effect.

It is important to state that the kinetic calibration method, using on-fiber standard or stable isotope method was also developed on the basis of the symmetric relationship between absorption and desorption process (Chen and Pawliszyn, 2004; Cui et al., 2013). However, this calibration method was widely used for sampling aqueous and gaseous systems when external matrix-matched calibration methods were difficult to apply, sample matrix was complicated, or analytes equilibration time was too long. In addition, the method had implicit challenges such as difficulty in obtaining deuterated or  $^{13}\text{C}$ -labeled compounds to be used as internal standards, which can be very expensive. Subsequently, provision was made by developing the one-calibrant (Ouyang et al., 2009) and standard-free (Ouyang et al., 2008) calibration methods for aqueous sampling to address the issue with the internal standards. However, no research work has been carried out when it comes to thorough studies on sampling from semi-solid samples.

In this study, firstly, we studied the sampling kinetic process of SPME for semi-solid samples and proposed a new theoretical model based on

diffusion to describe the extraction kinetic process. The effect of sample tortuosity and binding matrix on the kinetic process was further investigated. Subsequently, an on-fiber standard calibration method with internal standards was proposed for SPME semi-solid tissue quantitative analysis of polyaromatic hydrocarbons (PAHs) and polychlorinated biphenyls (PCBs) from agarose gel and fish tissue. The proposed calibration method can not only calibrate the complex matrix effect on tissue sampling, but also significantly reduce the number of internal standards that are either expensive or difficult to obtain. Subsequently, a large range of HOCs can be accurately quantified from single SPME sampling.

## 2. Materials and methods

### 2.1. Materials

Solid PAHs including acenaphthene (ACE), fluorene (FLU), phenanthrene (PHE), anthracene (ANT), fluoranthene (FLA), pyrene (PYR), and HPLC grade dichloromethane (DCM) were obtained from Sigma-Aldrich (Shanghai, China). PCBs including 2-chlorobiphenyl, pentachlorobenzene, 4-chlorobiphenyl, 2,5-dichlorobiphenyl, hexachlorobenzene, 3,3'-dichlorobiphenyl, 2,2',5-trichlorobiphenyl, 3,3',4,4'-tetrachlorobiphenyl were purchased from J&K Scientific (Beijing, China). Stock solution was prepared by dissolving known amounts of PAHs and PCBs in DCM to obtain  $5000\text{ mg L}^{-1}$  and  $1000\text{ mg L}^{-1}$ , respectively. Agarose gel was prepared to mimic the semi-solid tissue, while the bovine serum albumin (BSA) was selected as a model complex matrix. Both agar powder and BSA were obtained from Sigma-Aldrich. An SYLGARD 184 silicone elastomer kit purchased from Dow Corning (Shanghai, China) was used to prepare a standard gas generation vial. Homemade polydimethylsiloxane (PDMS) fiber (1 cm) with a thickness of  $44\text{ }\mu\text{m}$ , and  $0.18\text{ }\mu\text{L}$  volume were used for the SPME experiments. The detailed procedure for the preparation of PDMS fibers can be found in the literature (Xu et al., 2014a). Fish sample used in the experiments was purchased from the local supermarket.

An Agilent 6890 gas chromatography (GC) coupled with a 5975 mass spectrometry (MS) (CA, USA) was used for analytes separation and quantification. Chromatographic separation was attained on a HP-5MS ( $30\text{ m} \times 0.25\text{ mm I.D.} \times 0.25\text{ }\mu\text{m}$ ) fused silica column from Agilent, using helium as the carrier gas. Identification and quantification was obtained with the mass spectrometer in SIM mode. The selected ions were 128, 154, 166, 178, 178, 202 and 202 for NAP, ACE, FLU, PHE, ANT, FLA, PYR, respectively. Besides, a GERSTEL Multi-Purpose System (MPS) was applied for the automation process (Mülheim an der Ruhr, German).

### 2.2. Preparation of agarose gel simulation sample

Agarose gel has been widely used to study the diffusion mechanism of chemicals in semi-solid tissue due to the similarity of porous structures in both matrices (Nicholson and Phillips, 1981; Togunde et al., 2012; Zhang et al., 2011a; Zhou et al., 2008). However, agarose gel alone only mimic the diffusion path (tortuosity) of tissue without considering the effect of the binding matrix (Togunde et al., 2012). Therefore, BSA was added to mimic the protein binding in tissue. The detailed preparation of 0.8% agarose gel with different concentrations of BSA was described in our previous paper (Jiang et al., 2015c). Briefly, 0.80 g of agar powder was dissolved in 90 mL phosphate-buffered saline (PBS) buffer, and hand-shaken thoroughly before incubating at  $90\text{ }^\circ\text{C}$  in a water bath for 30 min. After that, the solution was transferred to another water bath at  $45\text{ }^\circ\text{C}$  and incubated for another 20 min. Subsequently, 10 mL PBS buffer with different concentrations of BSA were added, and the mixture was hand-shaken thoroughly. After 2 min mixing, 8.00 g of the mixture was transferred into 10 mL sampling vial. The mixture was cooled at room temperature for at least 3 h before being used within a 24 h period.

Two types of agarose gel with BSA were prepared. A type consisted of different concentrations of gel (0.5%, 0.8%, 1.5%, and 3.0%) but with constant concentration of BSA (1%) was used for mimicking tissues with different tortuosity. The other type was prepared with 0.8% of agarose gel but with varying BSA concentrations (0%, 0.5%, 1%, 2%, and 3%) was used to mimic the tissue with different concentrations of binding matrix.

### 2.3. Fish sample preparation

Real fish sample was used to validate the proposed kinetic model. The fish obtained from the local supermarket was cultured in the lab in deionized water for a week to ensure non-detectable background of PAHs and PCBs in the fish tissue. Prior to the analysis, if PAHs and PCBs were detected in the fish tissue, that batch of fish would be further cultured or a new batch of fish were purchase from another supermarket. For the actual experiments, the fish was firstly euthanized then, the tissue of interest was removed and homogenized in a blender. Finally, 8 g of the homogenized fish tissue were transferred to a 10 mL sampling vial using a thick glass rod.

### 2.4. Desorption time profiles of PAHs in agarose gel simulation sample

Sorption time profiles were usually conducted to study the analytes kinetic process of the extraction. The profiles can be obtained through the extraction of analytes from the samples spiked with constant concentrations of targeted compounds for different periods of time. However, it can be very difficult to guarantee that the targeted amounts of the compounds spiked into the agarose gel matrices were evenly distributed. In this study therefore, the desorption time profile was carried out to investigate the SPME kinetic process since extraction and desorption processes are isotropic (Chen and Pawliszyn, 2004). The SPME desorption experiment was carried out by first pre-loading the fiber with a constant amount by means of a standard gas generator, which was constructed according to the previously published work (Jiang et al., 2015a). After loading the fiber with PAHs, they were desorbed in the sample matrices at a pre-determined time intervals, and the amount left on the fiber was quantified by GC/MS. All the SPME experiments in the current study were carried out using the GERSTEL MPS autosampler with MAESTRO software. The automation process minimized the experimental error since there were no human interventions and thus increased the efficiency. Desorption time profiles were obtained for 7 PAHs in 8 types of simulation samples and 2 fish samples.

### 2.5. Statistical analysis and quality control

The data was processed with GraphPad Prism 7.0. The desorption rate constants were obtained from the time profiles with each sampling point performed in triplicate. A liquid injection calibration curve was conducted to obtain the relationship between the GC/MS peak area and the PAHs injection amount. The correlation coefficient of the calibration curves for all the compounds was higher than 0.99. The stability of the standard gas generator to provide consistent amounts of PAHs was monitored by direct sampling without fiber exposure to the sample matrix. The stability of the instrument was also monitored by injecting a quality control standard solution after every 9 sample injections.

## 3. Results and discussion

### 3.1. Kinetics of analytes in a semi-solid sample during sampling

The previous study (Xu et al., 2016b) demonstrated that the kinetic model of SPME sampling procedure in a semi-solid sample does not follow the first-order kinetic process because there is no bulk movement within the samples, convection mass transfer was negligible and diffusion processes dominated the mass transfer of analytes. When pre-

loaded SPME liquid coating (like PDMS) was exposed to a sample matrix, the extracted chemicals desorbed from the fiber and diffused to the sample matrix (Xu et al., 2016b). The concentration profile of chemicals on the fiber and in the sample matrix can be depicted as shown in Fig. 1, which revealed no clear diffusive boundary layer between two different phases in direct contact. This is different from what is observed for aqueous or gaseous systems, where the boundary layer exists with constant thickness between the sample matrix and fiber coating surface. According to Fick's diffusion law, the desorption amount of chemicals from the fiber ( $q_f(t)$ ) and the amount in the sample matrix ( $n_s(t)$ ) can be described by Eqs. (1) and (2). Detailed derivation of the equations can be found in the book published by Schwarzenbach (Schwarzenbach et al., 2003).

$$q_f(t) = \left(\frac{1}{\pi}\right)^{\frac{1}{2}} (D_f t)^{\frac{1}{2}} (C_f^0 - C_{f/s}) \quad (1)$$

$$n_s(t) = \left(\frac{1}{\pi}\right)^{\frac{1}{2}} (D_s t)^{\frac{1}{2}} (C_{s/f} - C_s^0) \quad (2)$$

where  $C_f^0$  and  $C_s^0$  are the initial concentration of chemicals on the fiber and in the sample, respectively.  $C_{f/s}$  and  $C_{s/f}$  are the concentrations at both sides of coating surface relative to the sample.  $D_f$  and  $D_s$  are diffusion coefficients in fiber coating and sample, respectively. By integrating the Eqs. (1) and (2), given that  $K_{fs} = \frac{C_{f/s}}{C_{s/f}}$  resulted in Eq. (3).

$$q_f(t) = \left(\frac{t}{\pi}\right)^{1/2} \frac{C_f^0 - C_s^0 / K_{fs}}{\frac{1}{D_f^{1/2}} + \frac{K_{fs}}{D_s^{1/2}}} \quad (3)$$

when

$$\frac{1}{D_f^{1/2}} \ll \frac{K_{fs}}{D_s^{1/2}} \quad (4)$$

$$q_f(t) = \left(\frac{t D_s}{\pi}\right)^{\frac{1}{2}} \left(\frac{C_f^0}{K_{fs}} - C_s^0\right) \quad (5)$$

When  $C_s^0 = 0$ , Eq. (5) can be rearranged to Eq. (6).

$$\frac{q_f(t)}{q_f^0} = \left(\frac{D_s}{\pi}\right)^{\frac{1}{2}} \frac{1}{K_{fs} V_f} t^{1/2} \quad (6)$$

$$\frac{Q_f(t)}{q_f^0} = -\left(\frac{D_s}{\pi}\right)^{\frac{1}{2}} \frac{1}{K_{fs} V_f} t^{\frac{1}{2}} + 1 \quad (7)$$

Let

$$a = \left(\frac{D_s}{\pi}\right)^{\frac{1}{2}} \frac{1}{K_{fs} V_f} \quad (8)$$

$$\frac{Q_f(t)}{q_f^0} = (a) t^{\frac{1}{2}} + 1 \quad (9)$$

$Q_f(t)$  is the amount of chemical left on the fiber after desorption. Eq. (9) indicates that  $\frac{Q_f(t)}{q_f^0}$  is linearly correlated to  $t^{\frac{1}{2}}$  in the same sample matrix, and the slope of the curve equals,  $\left(\frac{D_s}{\pi}\right)^{\frac{1}{2}} \frac{1}{K_{fs} V_f}$ , which can be defined as desorption time constant ( $a$ ).

Different from the first-order kinetic equation, in which the desorption amount and the desorption time are defined to be an exponential relationship, the currently proposed model shows a linear relationship between the desorption amount and the square root of desorption

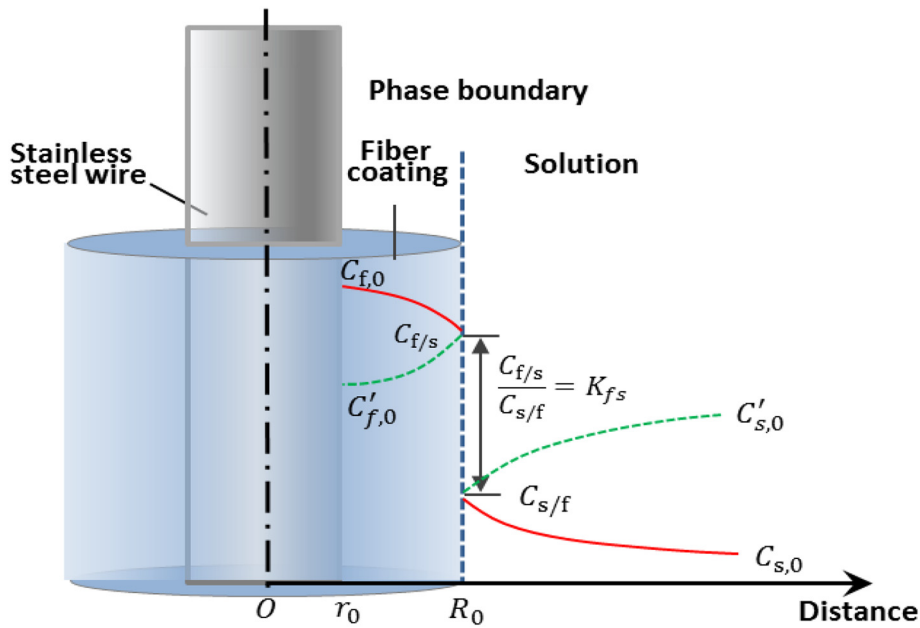


Fig. 1. Concentration profiles of chemicals between SPME coating and semi-solid coating. Red solid curve, desorption process; green dashed, extraction process.

time. Results showed that Eq. (9) had much better fitting coefficients (higher than 0.9605, Fig. 2) compared to the ones fitted by the first-order equation, which were 0.9181, 0.7656 and 0.8327 for ACE, PHE, and PYR, respectively (Fig. S1). The fitting coefficients from the proposed model for NAP, FLU, ANT, and FLA were 0.9857, 0.9730, 0.9293 and 0.9807, respectively, which were in excellent agreement with the proposed model.

3.2. Effect of the sample matrix on the desorption time constant

The slopes of the curves in Fig. 2 correlated to the desorption time constant (*a*) of the analytes during SPME process, and also indicate how fast the desorption process reaches equilibrium. The desorption time constants of the 7 PAHs in the different sample matrices are shown in Table 1. As shown, the desorption time constant decreased as the concentration of agarose gel increased, while increasing with increase in the BSA concentration. In addition, the time constant was observed to decrease as the hydrophobicity of the compound increased.

Table 1 also shows the desorption time constants of the 7 PAHs in different concentrations of agarose gel with a constant BSA concentration. Since the amount of agarose gel determined the tortuosity of the sample matrix, changes in desorption time constants in the samples with varying concentrations of agarose gel indicated that the tortuosity of the sample influences the sampling kinetic process. According to literature, the tortuosity determined the diffusion path of the chemicals and the diffusion coefficient. Effective diffusion coefficient in a non-aqueous sample (*D<sub>s</sub>*) can be corrected by the parameter of tortuosity (*τ*). *D<sub>s</sub>* is the diffusion coefficient in aqueous (*D<sub>u</sub>*) divided by *τ*<sup>2</sup> (Schwarzenbach et al., 2003). Accordingly, the effective diffusion coefficient decreased as the tortuosity increased. Based on Eq. (8), decrease of diffusion coefficient result in a decrease in the desorption time constants. Thus, higher tortuosity causes decrease in the desorption time constant and the kinetic process. Table 1 shows the experimental results, which were in agreement with the proposed theory.

Table 1 also shows the effect of complex matrix on the sampling kinetic process. The presence of BSA not only significantly enhanced the desorption time constants, but also increases as the concentration of BSA increased. The underlying principle can be explained by re-writing Eq. (8) follows:

$$a = \left(\frac{D_s}{\pi}\right)^{\frac{1}{2}} \frac{1}{K_{fs} V_f} = \left(\frac{D_s}{\pi}\right)^{\frac{1}{2}} \frac{1}{V_f K_{ff}} (K_{BSA} C_{BSA} + 1) \tag{10}$$

where *K<sub>ff</sub>* is the distribution coefficient of the chemicals between fiber coating and sample without complex matrix, while *K<sub>fs</sub>* is the distribution

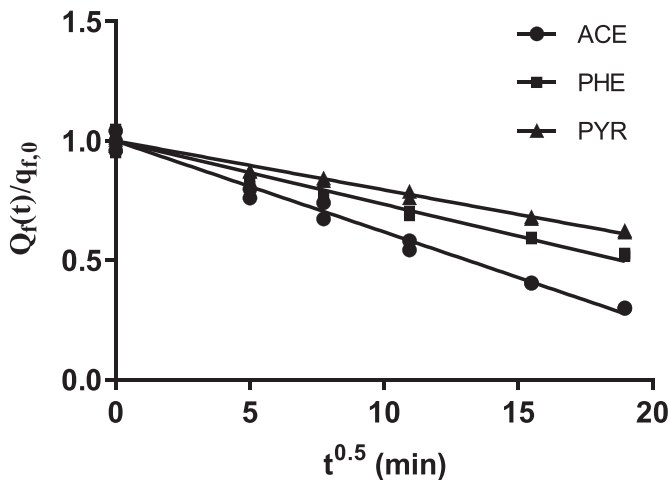


Fig. 2. Desorption time profiles of PAHs in the sample with 1.5% agarose gel and 1% BSA fitted by Eq. (7).

Table 1 Desorption time constants of PAHs in different ratios of gel with 1% BSA and in 0.8% gel with different concentrations of BSA.

<i>a</i>	1% BSA, diff. gel%			0.8% gel, diff. BSA%					logK <sub>ow</sub>
	0.8%	1.5%	3.0%	0.0%	0.5%	1.0%	2.0%	3.0%	
NAP	0.058	0.054	0.044	0.039	0.058	0.064	0.067	0.075	3.37
ACE	0.039	0.035	0.032	0.023	0.030	0.039	0.047	0.054	4.07
FLU	0.034	0.031	0.027	0.021	0.027	0.034	0.042	0.048	4.18
PHE	0.026	0.024	0.021	0.016	0.021	0.026	0.036	0.038	4.46
ANT	0.024	0.022	0.020	0.015	0.019	0.024	0.033	0.037	4.50
PLA	0.020	0.021	0.020	0.009	0.017	0.020	0.031	0.034	4.90
PYR	0.018	0.019	0.017	0.008	0.017	0.018	0.030	0.031	4.88



coefficient between fiber coating and sample with complex matrix,  $K_{fs}$  =  $K_{ff} \times \frac{1}{K_{BSA} C_{BSA} + 1}$  (Jiang et al., 2015c).  $K_{BSA}$  is the distribution coefficient between complex matrix and sample, and  $C_{BSA}$  is the concentration of complex matrix.

For samples with constant gel and different concentrations of BSA, the diffusion coefficient ( $D_s$ ), and the distribution coefficients ( $K_{ff}$  and  $K_{BSA}$ ) were constant. According to Eq. (10), the desorption time constant was linearly proportional to the concentration of the complex matrix ( $C_{BSA}$ ) in the sample. This is clearly demonstrated in Fig. 3 where the experimental results agreed well with the theoretical prediction. The results imply that different tissues with different amount of lipid cannot have the same sampling rate. Thus, when using an external calibration method, the calibration curve should be obtained using exact matrix match.

### 3.3. Calibration method based on the newly proposed kinetic model

The main purpose of studying the kinetic process of SPME applied to semi-solid was to develop a reliable calibration method, which will also provide better understanding of the kinetic processes of analytes in tissues during the sampling process. The proposed calibration method was used to show there is a direct linear correlation between the extracted amount and the analytes concentration in the sample due to isotropy. According to the proposed SPME kinetic model, the extracted amount of the analytes in the semi-solid sample can be described by Eq. (11). Detailed derivation can be found in SI.

$$\frac{n_f(t)}{n_f^{eq}} = \left(\frac{D_s}{\pi}\right)^{\frac{1}{2}} \frac{1}{K_{fs} V_f} t^{\frac{1}{2}} \quad (11)$$

where  $n_f(t)$  and  $n_f^{eq}$  are the amount extracted after  $t$  min exposure and the equilibrium extracted amount, respectively. The extracted time constant,  $a = \left(\frac{D_s}{\pi}\right)^{\frac{1}{2}} \frac{1}{K_{fs} V_f}$ , is the same as the desorption time constant (Eq. (8)). By knowing the extraction time constant, and the extracted amount ( $n_f(t)$ ), Eq. (11) can be used to calculate the equilibrium extracted amount,  $n_f^{eq}$ . For *in vivo* SPME,  $n_f^{eq} = K_{fs} V_f C_s^0$ , where  $C_s^0$  is the original concentration of analytes in the sample. Since the desorption process is being used for quantification, it is worth noting that there is isotropic relation between the extraction and desorption processes of the analytes. This is demonstrated by combining Eqs. (7) and (11), which then gives the new expression,  $\frac{Q_f(t)}{q_f^0} + \frac{n_f(t)}{n_f^{eq}} = 1$ , indicating isotropic relationship between extraction and desorption process. This

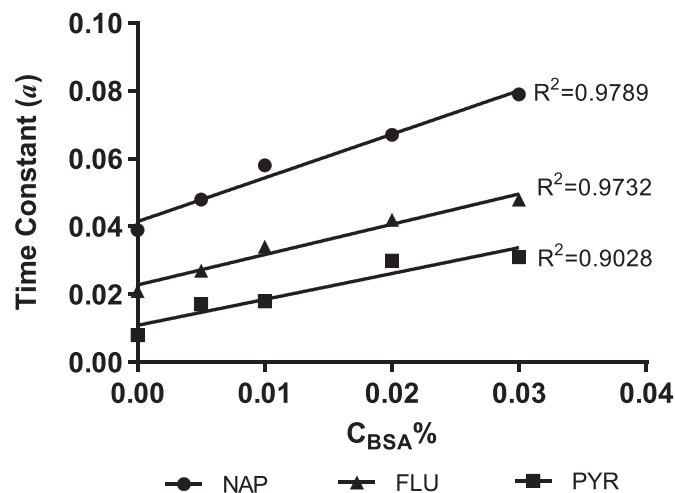


Fig. 3. The linear correlation between desorption time constants ( $a$ ) and concentration of complex matrix ( $C_{BSA}$ ).

relationship in agarose gel and fish tissue was also experimentally demonstrated in literature (Togunde et al., 2012; Xu et al., 2016b; Zhang et al., 2011a).

It is important to state also that compounds that demonstrate isotropic relationship for the extraction and desorption process, will also have the same time constants for both processes. The calibration methods of on-fiber standard calibration or the PRC calibration method (Chen and Pawliszyn, 2004; Cui et al., 2013) was developed based on the isotropic relationship for the extraction and desorption process. The deuterated compounds can be used as internal standards to obtain the time constants of target analytes. Theoretically, internal standards for all the target analytes should be obtained when using this method. However, the calibration method can also be used with fewer internal standards.

The underlying principle of being able to use fewer internal standards is because of the relationship between the time constants and the physiochemical properties such as the diffusion coefficients of the targeted compounds. From Table 1, the desorption time constants decreased as the hydrophobicity of the compounds increased in the same sample matrix. However, no clear relationship was found between the desorption time constants and the  $K_{ow}$  of the compounds. Instead, there was a very good linear correlation between the desorption time constants and the square root of diffusion coefficients of compounds. Since the diffusion coefficient can be described by molar volume of compounds,  $D_u = \frac{2.3 \times 10^{-4}}{\bar{V}_i^{0.71}}$  (Schwarzenbach et al., 2003), the relationship between the time constant and diffusion coefficient can be rewritten as Eq. (12). Time constant ( $a$ ) was linearly proportional to the  $1/\bar{V}_i^{0.355}$  and the linearity of each analyte was within the range 0.9542 to 0.9929 for all 7 PAHs in the different sample matrices (Fig. S2).

$$a = \left(\frac{2.3 \times 10^{-4}}{\pi r^2 \bar{V}_i^{0.71}}\right)^{\frac{1}{2}} \frac{1}{K_{fs} V_f} \quad (12)$$

The significance of the relationship between time constants and the diffusion coefficients of compounds was that fewer calibrants could be used successfully for on-fiber standard calibration since the time constants of compounds, even without internal standards, can be calculated from their molar volumes. Also the desorption time constants of 8 PCBs in agarose gel with 3% BSA was determined to further investigate whether the above relationship can be extended to different groups of compounds. The desorption time constants of PCBs together with the ones for 7 PAHs were plotted with the values of  $1/\bar{V}_i^{0.355}$  for each compound. A linear curve with relatively good regression (Fig. 4) was also

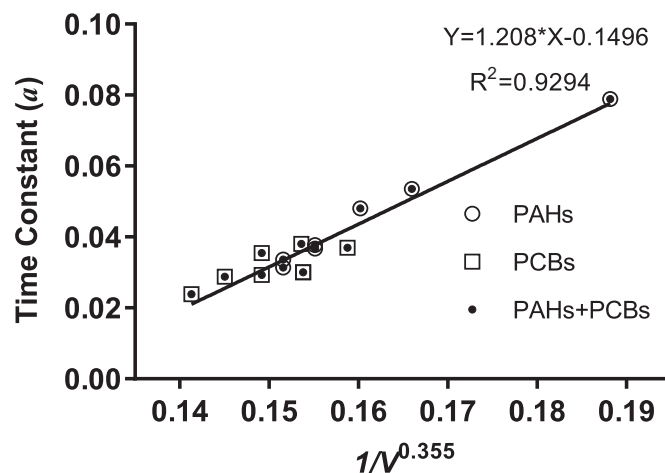


Fig. 4. The linear relationship between desorption time constants and molar volume of 7 PAHs and 8 PCBs in 0.8% gel with 3% BSA.

observed, demonstrating the applicability of the linear relationship between different groups of compounds.

The linear relationship between time constants and diffusion coefficient can be further explained from Eq. (10), in which  $K_{BSA}C_{BSA} + 1$  can be simplified into  $K_{BSA}C_{BSA}$  when  $K_{BSA}C_{BSA} \gg 1$ . That implies, the  $a$  value will be linearly dependent on  $\sqrt{D_s}$  if the ratio,  $K_{BSA}/K_{ff}$  was constant.  $K_{BSA}$  and  $K_{ff}$  are defined as the partition coefficients of organic compounds in BSA and PDMS fiber coating respectively. In literature, both values have been well studied and linear correlations between these values and the  $K_{ow}$  were commonly observed. For example, Mayer et al. (2000) reported a linear correlation  $K_{ff} = 0.123K_{ow}$  for PAHs, PCBs and pesticides with  $\log K_{ow}$  ranging from 4.47 to 7.51. In the article published by Endo et al., (Endo and Goss, 2011), a linear correlation  $K_{BSA} = 0.200K_{ow}^{1.01}$  was also found for the compounds with  $\log K_{ow} \leq 5$ . Similar correlation also found for the partition coefficients between dissolved organic carbon (DOM) or lipid content and water. Burkhard (Burkhard, 2000) summarized >70 references and observed a relationship of  $K_{DOM} = 0.08K_{ow}$  at 95% confidence limits by a factor of 20 in either direction, while Endo (Endo et al., 2011) summarized the partition coefficients of 156 neutral organic compounds between liposomes and water, and found the correlation of  $\log K_{lip, w} = (1.01 \pm 0.02) \log K_{ow} + (0.12 \pm 0.07)$ . The above reported correlation also indicate that the ratio of  $K_{matrix}/K_{ff}$  is constant, which was also demonstrated by Pei reporting a relative constant value of  $K_{protein, lipid}/K_{PDMS}$  for compounds with  $K_{ow}$  values that extend to more than six orders of magnitude (Pei et al., 2017). It is worth to note that, although the linear relationship between time constants and diffusion coefficient can be applied for compounds with a large range of  $K_{ow}$ , it may not work for the compounds with kinetic parameters that cannot meet the criteria of Eq. (4).

#### 3.4. Application of proposed calibration method for fish tissue sampling

The concept of the linear correlation between time constants and the molar volume of the compounds was further applied to quantitative analysis of PAHs and PCBs in real tissue sampling. The desorption time profiles of 7 PAHs and 8 PCBs in fish tissue were obtained, and the desorption time constants were obtained by fitting the profiles with the proposed model (Eq. (7)). As shown in Fig. 5, there was linear correlation between desorption time constant and  $1/\bar{V}_i^{0.355}$  found for all PAHs and PCBs in both tilapia belly and back tissue with coefficients of 0.8411 and 0.8653, respectively. This result demonstrates the feasibility of the proposed kinetic model and the developed on-fiber standard calibration method with fewer calibrants for quantitative analysis of semi-solid samples.

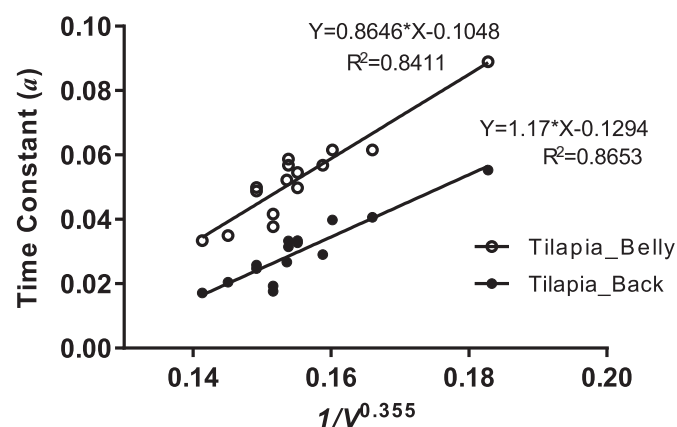


Fig. 5. The linear relationship between desorption time constant and molar volume of 7 PAHs and 8 PCBs in Tilapia tissue.

#### 4. Conclusion

Application of a proper calibration method is very critical when using non-exhaustive sampling techniques like SPME for quantitative analysis. In this study, we proposed a new theoretical model to further provide a better understanding of the sampling kinetics of the analytes during SPME in the semi-solid sample. The model well explained the effect of binding matrix and tortuosity on the SPME tissue sampling. Based on the model, the relationship between the sampling kinetic parameters and the properties of the targeted compounds was established, and a novel on-fiber standard calibration method with fewer calibrants was developed to quantify PAHs and PCBs in tissue sample. The calibration method can be applied to very complex tissue sample with fewer internal standards at a relatively lower cost. In addition, as a green analytical method for environmental sampling, current proposed method extended the green aspects of the SPME. The proposed sampling kinetic model provides the theoretical foundation for SPME semi-solid sampling, while the calibration method will promote the wide application of *in vivo* SPME.

#### Notes

The authors declare no competing financial interest.

#### Acknowledgments

We acknowledge financial support from the projects of the National Natural Science Foundation of China (21777058, 21737006).

#### Appendix A. Supplementary data

Supporting information includes three figures and a text paragraph showing the mathematical deduction process for the kinetic equation for SPME semi-solid sampling. Supplementary data to this article can be found online at <https://doi.org/10.1016/j.scitotenv.2018.11.226>.

#### References

- Augusto, F., Luiz Pires Valente, A., 2002. Applications of solid-phase microextraction to chemical analysis of live biological samples. *TrAC Trends Anal. Chem.* 21, 428–438. [https://doi.org/10.1016/S0165-9936\(02\)00602-7](https://doi.org/10.1016/S0165-9936(02)00602-7).
- Bessonneau, V., Ings, J., McMaster, M., Smith, R., Bragg, L., Servos, M., Pawliszyn, J., 2017. In vivo microsampling to capture the elusive exposome. *Sci. Rep.* 7 (44038). <https://doi.org/10.1038/srep44038>.
- Burkhard, L.P., 2000. Estimating dissolved organic carbon partition coefficients for non-ionic organic chemicals. *Environ. Sci. Technol.* 34, 4663–4668.
- Chen, Y., Pawliszyn, J., 2004. Kinetics and the on-site application of standards in a solid-phase microextraction fiber. *Anal. Chem.* 76, 5807–5815. <https://doi.org/10.1021/ac0495081>.
- Chen, G., Jiang, R., Qiu, J., Cai, S., Zhu, F., Ouyang, G., 2015. Environmental fates of synthetic musks in animal and plant: an in vivo study. *Chemosphere* 138, 584–591. <https://doi.org/10.1016/j.chemosphere.2015.07.003>.
- Cui, X., Bao, L., Gan, J., 2013. Solid-phase microextraction (SPME) with stable isotope calibration for measuring bioavailability of hydrophobic organic contaminants. *Environ. Sci. Technol.* 47, 9833–9840. <https://doi.org/10.1021/es4022987>.
- Endo, S., Goss, K.-U., 2011. Serum albumin binding of structurally diverse neutral organic compounds: data and models. *Chem. Res. Toxicol.* 24, 2293–2301. <https://doi.org/10.1021/tx200431b>.
- Endo, S., Escher, B.L., Goss, K.U., 2011. Capacities of membrane lipids to accumulate neutral organic chemicals. *Environ. Sci. Technol.* 45, 5912–5921. <https://doi.org/10.1021/es200855w>.
- Jiang, R., Lin, W., Wen, S., Zhu, F., Luan, T., Ouyang, G., 2015a. Development of a full automation solid phase microextraction method for investigating the partition coefficient of organic pollutant in complex sample. *J. Chromatogr. A* 1406, 27–33. <https://doi.org/10.1016/j.chroma.2015.06.018>.
- Jiang, R., Xu, J., Lin, W., Wen, S., Zhu, F., Luan, T., Ouyang, G., 2015b. Investigation of the kinetic process of solid phase microextraction in complex sample. *Anal. Chim. Acta* 900, 111–116. <https://doi.org/10.1016/j.aca.2015.09.010>.
- Jiang, R., Xu, J., Zhu, F., Luan, T., Zeng, F., Shen, Y., Ouyang, G., 2015c. Study of complex matrix effect on solid phase microextraction for biological sample analysis. *J. Chromatogr. A* 1411, 34–40. <https://doi.org/10.1016/j.chroma.2015.07.118>.
- Lord, H.L., Zhang, X., Musteata, F.M., Vuckovic, D., Pawliszyn, J., 2011. In vivo solid-phase microextraction for monitoring intravenous concentrations of drugs and metabolites. *Nat. Protoc.* <https://doi.org/10.1038/nprot.2011.329>.

- Mayer, P., Vaes, W.H.J., Hermens, J.L.M., Oomen, A.G., Tolls, J., 2000. Absorption of hydrophobic compounds into the poly(dimethylsiloxane) coating of solid-phase microextraction fibers: high partition coefficients and fluorescence microscopy images. *Anal. Chem.* 72, 459–464. <https://doi.org/10.1021/ac990948f>.
- Nicholson, B.Y.C., Phillips, J.M., 1981. Ion diffusion modified by tortuosity and volume fraction in the extracellular microenvironment of the rat cerebellum. *J. Physiol.* 321, 225–257.
- Ouyang, G., Cai, J., Zhang, X., Li, H., Pawliszyn, J., 2008. Standard-free kinetic calibration for rapid on-site analysis by solid-phase microextraction. *J. Sep. Sci.* 31, 1167–1172. <https://doi.org/10.1002/jssc.200700495>.
- Ouyang, G., Cui, S., Qin, Z., Pawliszyn, J., 2009. One-calibrant kinetic calibration for on-site water sampling with solid-phase microextraction. *Anal. Chem.* 81, 5629–5636. <https://doi.org/10.1021/ac900315w>.
- Ouyang, G., Oakes, K.D., Bragg, L., Wang, S., Liu, H., Cui, S., Servos, M.R., Dixon, D.G., Pawliszyn, J., 2011a. Sampling-rate calibration for rapid and nonlethal monitoring of organic contaminants in fish muscle by solid-phase microextraction. *Environ. Sci. Technol.* 45, 7792–7798. <https://doi.org/10.1021/es201709j>.
- Ouyang, G., Vuckovic, D., Pawliszyn, J., 2011b. Nondestructive sampling of living systems using in vivo solid-phase microextraction. *Chem. Rev.* 111, 2784–2814. <https://doi.org/10.1021/cr100203t>.
- Pawliszyn, J., 2012. *Handbook of Solid Phase Microextraction*. Elsevier, UK.
- Pei, Y., Li, H., You, J., 2017. Determining equilibrium partition coefficients between lipid/protein and polydimethylsiloxane for highly hydrophobic organic contaminants using preloaded disks. *Sci. Total Environ.* 598, 385–392. <https://doi.org/10.1016/j.scitotenv.2017.04.123>.
- Roszkowska, A., Tascon, M., Bojko, B., Goryński, K., dos Santos, P.R., Cypel, M., Pawliszyn, J., 2018a. Equilibrium ex vivo calibration of homogenized tissue for in vivo SPME quantitation of doxorubicin in lung tissue. *Talanta* 183, 304–310. <https://doi.org/10.1016/j.talanta.2018.02.049>.
- Roszkowska, A., Yu, M., Bessonau, V., Bragg, L., Servos, M.R., Pawliszyn, J., 2018b. Metabolome profiling of fish muscle tissue exposed to benzo[a]pyrene using in vivo solid-phase microextraction. *Environ. Sci. Technol. Lett.*, 431–435 <https://doi.org/10.1021/acs.estlett.8b00272>.
- Schwarzenbach, R.P., Gschwend, P.M., Imboden, D.M., 2003. *Environmental Organic Chemistry*. Second ed. John Wiley & Sons, Inc.
- Togunde, O.P., Oakes, K., Servos, M., Pawliszyn, J., 2012. Study of kinetic desorption rate constant in fish muscle and agarose gel model using solid phase microextraction coupled with liquid chromatography with tandem mass spectrometry. *Anal. Chim. Acta* 742 (2–9). <https://doi.org/10.1016/j.aca.2011.12.034>.
- Xu, J., He, S., Jiang, R., Zhu, F., Ruan, J., Liu, H., Luan, T., Ouyang, G., 2014a. Disposable solid-phase microextraction fiber coupled with gas chromatography-mass spectrometry for complex matrix analysis. *Anal. Methods* 6, 4895–4900. <https://doi.org/10.1039/c4ay00230j>.
- Xu, J., Luo, J., Ruan, J., Zhu, F., Luan, T., Liu, H., Jiang, R., Ouyang, G., 2014b. In vivo tracing uptake and elimination of organic pesticides in fish muscle. *Environ. Sci. Technol.* 48, 8012–8020.
- Xu, J., Huang, S., Jiang, R., Cui, S., Luan, T., Chen, G., Qiu, J., Cao, C., Zhu, F., Ouyang, G., 2016a. Evaluation of the availability of bound analyte for passive sampling in the presence of mobile binding matrix. *Anal. Chim. Acta* 917, 19–26. <https://doi.org/10.1016/j.aca.2016.02.039>.
- Xu, J., Huang, S., Wei, S., Yang, M., Cao, C., Jiang, R., Zhu, F., Ouyang, G., 2016b. Study on the diffusion-dominated solid-phase microextraction kinetics in semisolid sample matrix. *Anal. Chem.* 88, 8921–8925. <https://doi.org/10.1021/acs.analchem.6b02673>.
- Zhang, X., Oakes, K.D., Cui, S., Bragg, L., Servos, M.R., Pawliszyn, J., 2010a. Tissue-specific in vivo bioconcentration of pharmaceuticals in rainbow trout (*Oncorhynchus mykiss*) using space-resolved solid-phase microextraction. *Environ. Sci. Technol.* 44, 3417–3422. <https://doi.org/10.1021/es903064t>.
- Zhang, X., Oakes, K.D., Luong, D., Wen, J.Z., Metcalfe, C.D., Pawliszyn, J., Servos, M.R., 2010b. Temporal resolution of solid-phase microextraction: measurement of real-time concentrations within a dynamic system. *Anal. Chem.* 82, 9492–9499. <https://doi.org/10.1021/ac102186u>.
- Zhang, X., Oakes, K.D., Hoque, E., Luong, D., Metcalfe, C.D., Pawliszyn, J., Servos, M.R., 2011a. Pre-equilibrium solid-phase microextraction of free analyte in complex samples: correction for mass transfer variation from protein binding and matrix tortuosity. *Anal. Chem.* 83, 3365–3370.
- Zhang, X., Oakes, K.D., Luong, D., Metcalfe, C.D., Pawliszyn, J., Servos, M.R., 2011b. Kinetically-calibrated solid-phase microextraction using label-free standards and its application for pharmaceutical analysis. *Anal. Chem.* 83, 2371–2377. <https://doi.org/10.1021/ac200032k>.
- Zhou, S.N., Zhao, W., Pawliszyn, J., 2008. Kinetic calibration using dominant pre-equilibrium desorption for on-site and in vivo sampling by solid-phase microextraction. *Anal. Chem.* 80, 481–490. <https://doi.org/10.1021/ac701871q>.